Research Report

98-52

A Dual Three-Phase Drive System with a Reduced Switch Count

E. Ledezma, A. Munoz-Garcia, T.A. Lipo

Wisconsin Power Electronic Research Center
University of Wisconsin-Madison
Madison WI 53706-1691

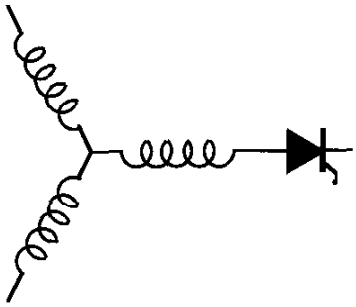

Wisconsin
Electric
Machines &
Power
Electronics
Consortium

University of Wisconsin-Madison
College of Engineering
Wisconsin Power Electronics Research Center
2559D Engineering Hall
1415 Engineering Drive
Madison WI 53706-1691

IAS Conference Records. pp. 781-788. October 1998.

A Dual Three-Phase Drive System with a Reduced Switch Count

E. Ledezma A. Muñoz-Garcia T. A. Lipo
Department of Electrical and Computer Engineering
University of Wisconsin – Madison
1415 Engineering Drive
Madison, WI 53706-1691 USA

***Abstract*-A dual CRPWM VSI based on multiple two-phase PWM inverters, also called a B4 topology, requiring a dual three-phase drive system with reduced switch count is proposed. The drive utilizes a total of only eight switches to produce two sets of three-phase sinusoidal output currents. This new scheme minimizes the single-phase current flow through the DC-link capacitors, which is a common problem in reduced switch count topologies. By controlling the phase and magnitude of the currents generated by each inverter it is possible to cancel out the single-phase current flow through the DC-link capacitors. The paper presents a mathematical model of the proposed dual motor drive system including a control strategy that minimizes the capacitor's voltage variations and the single-phase current flow through the DC-link capacitors. In order to verify the performance of the proposed drive system, an application on traction of an electric vehicle is carried out. The simulation results show that the single-phase current flow through the DC-link can be eliminated or minimized when the vehicle moves in a straight-line regime, turning regime, or slippage condition.**

I. INTRODUCTION

Due to the advances in power electronic technology, variable frequency AC drives are presently being broadly applied. Traditional AC drives are based on a three-phase inverter that is used to feed an induction motor; thus, a total of six switches are required. Reducing the number of active switches is desirable in applications where low cost, improved reliability and less conduction loss is of importance. Due to its many advantages, a number of studies have been conducted utilizing a reduced-switch count structure. For instance, a two-phase topology using a split DC-link capacitor and requiring only four switches was introduced in [1]. In addition, in [2] a B4 inverter employing only four switches is proposed as a viable alternative compared to the conventional six-switch converter. A detailed analysis of the harmonic losses and torque pulsations produced by a four-switch voltage controlled topology was carried out by Van Der Broeck et.al. [2,3]. This analysis showed that both copper losses and torque pulsations could be greatly reduced by instantaneously controlling the time shift between the two voltage pulses during the pulse period. A three-phase to three-phase VSI–PWM rectifier-inverter scheme with eight switches was proposed in [4]. This topology had the capability of delivering sinusoidal input currents with unity power factor and bi-directional power flow. The problem of voltage fluctuation in the DC-link, however, is a potential limitation for this eight-switch structure.

Drawbacks of the reduced-switch topologies also include increased voltage stress on both the power devices and the induction motor, increased switching losses due to a higher DC-link voltage, and single-phase circulating currents through the DC-link capacitors [5]. The problem of single-phase circulating currents through the DC-link capacitors is also addressed in [6]. A comparative study of a reduced-switch drive structure was conducted and applied to mobile robot motorization in [7]. However, the problem of the single-phase currents was not addressed, which is a common limitation of reduced-switch count topologies. In addition, the existence of large DC-link voltage variations due to, among other causes, the circulation of single-phase currents through the DC-link capacitor was discussed in [8], although a solution was not given.

In this paper a new dual AC drive system that minimizes the single-phase current flow through the DC-link capacitors, thus eliminating their voltage variation and extra losses, is introduced. The proposed drive system uses two four-switch inverters connected back to back which share a single split DC-link capacitor. The inverters are used to feed two induction motors that operate at the same fundamental frequency with a similar current level. To verify the performance of the proposed drive system, an application on traction of an electric vehicle is carried out. A mathematical model of the proposed AC drive is derived and applied through simulation.

II. SYSTEM CONFIGURATION AND PRINCIPLE OF OPERATION

The proposed drive system is schematically shown in Fig. 1. The drive consists of dual two-phase inverters connected back to back with a common DC bus, thus requiring only eight switches instead of the conventional twelve. The load corresponds to two induction machines that are fed from each inverter. It is assumed that the phase and magnitude of the load currents can be independently adjusted and that each inverter is operated under current control using hysteresis regulators. It is also assumed that the DC bus voltage is supplied by a rectifier (not shown for simplicity).

0-7803-4943-1/98/$10.00 © 1998 IEEE

In a two-phase inverter topology two of the machine's phases are connected to two poles of the inverter and the third phase is connected to the center point of the DC-link. Because there is no neutral connection and two of the line currents are regulated, the current through the third line is also regulated (sinusoidal). This configuration creates a single-phase current flow through the capacitors in the DC-link. By connecting a second two-phase inverter to the same DC bus it is possible to compensate for the single-phase current in the capacitors. This is achieved by adjusting the relative phase angle of the currents in the two inverters.

In order to eliminate the single-phase current, the relative phase of the currents in each inverter must be 180 degrees out of phase. The current through C_1 in Fig. 1 is given by

$$i_{cap1} = i_{cs} + i_{zs} + i_{cap2} \tag{1}$$

where i_{cs} and i_{zs} are the line currents and i_{cap2} is the current through C_2. From (1) it can be noted that if i_{cs} has the negative value $-i_{zs}$, then i_{cap1} will be equal to i_{cap2}. Therefore, they will total zero. As a consequence, the effective circulating current through the DC-link capacitors will be ideally zero. To develop actively this control strategy, the space complex vector dqo approach is utilized.

III. CONTROL STRATEGY TO MINIMIZE THE DC-LINK SINGLE-PHASE CURRENT CAPACITORS

In (1), to minimize the single-phase circulating current through the DC-link capacitors, the line currents i_{cs} and i_{zs} must be 180 degrees out of phase. This is accomplished by choosing the current references for inverter 1 as follows:

$$i^*_{as} = i^{e*}_{q_1} \cos\theta_{rf1} + i^{e*}_{d_1} \sin\theta_{rf1} \tag{2}$$

$$i^*_{bs} = i^{e*}_{q_1} \cos(\theta_{rf} - 120^\circ) + i^{e*}_{d_1} \sin\theta_{rf1}, \tag{3}$$

where $i^{e*}_{q_1}$ is the torque command, and $i^{e*}_{d_1}$ is the flux command in the synchronous reference frame. In the same fashion, the current references for inverter 2 are chosen as

$$i^*_{xs} = i_{q2rot} \cos\theta_{rf2} - i_{d2rot} \sin\theta_{rf2} \tag{4}$$

$$i^*_{ys} = i_{q2rot} (\cos\theta_{rf2} - 120^\circ) + i_{d2rot} (\sin\theta_{rf2} - 120^\circ). \tag{5}$$

In (4) and (5), i_{q2rot} and i_{d2rot} are chosen such that

$$i_{q2rot} = i^{e*}_{q_2} \cos\phi - i^{e*}_{d_2} \sin\phi \tag{6}$$

$$i_{d2rot} = i^{e*}_{q_2} \sin\phi + i^{e*}_{d_2} \sin\phi, \tag{7}$$

where $i^{e*}_{q_2}$ and $i^{e*}_{d_2}$ are the torque and flux commands for induction machine 2.

In (6) and (7), the angle ϕ is determined as indicated in the block diagram of Fig. 2. Here, i_{qs1}, i_{ds1}, i_{qs2} and i_{ds2} are the inputs measured stator currents in the stationary reference frame. The currents are transform to the synchronous reference frame utilizing the flux rotor position θ_{rfl} in both transformations in order to have the currents referred to a common frame of reference. After the transformations, the new currents i^e_{q1}, i^e_{d1}, i^e_{d2} and i^e_{q2} referred to the rotor flux frame of induction machine 1 are obtained. The position of the complex current vector for induction machine 1, ϕ_1, and induction machine 2, ϕ_2, are calculated utilizing the complex current components. Angles ϕ_1 and ϕ_2 become

$$\phi_1 = a\tan\left(\frac{i^e_{q_1}}{i^e_{d_1}}\right) \tag{8}$$

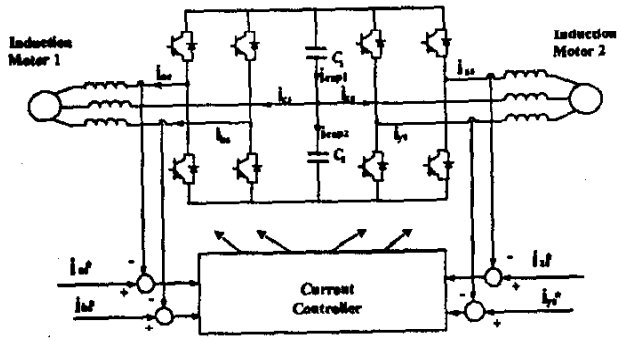

Fig. 1. Reduced switch count three-phase dual drive.

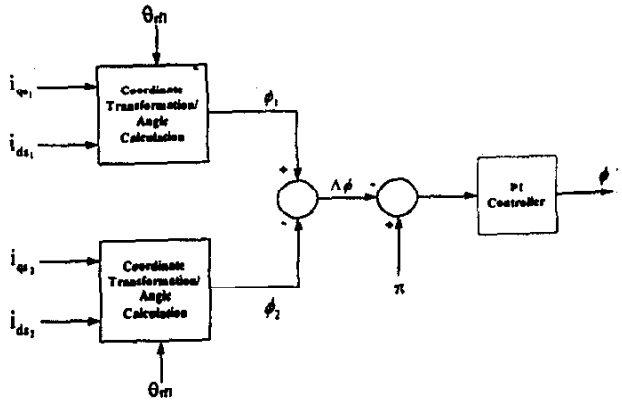

Fig. 2. Active calculation of the rotation angle ϕ.

$$\phi_2 = a\tan\left(\frac{i^e_{q_2}}{i^e_{d_2}}\right). \qquad (9)$$

Fig. 2 shows the active calculation process of the rotation angle ϕ. The error $\phi_1 - \phi_2 = \Delta\phi$ is calculated and compared to π and further processed through a PI-type controller. The actual angle ϕ is found as

$$\phi = K_{p\phi}(\pi - \Delta\phi) + K_{i\phi}\int_0 (\pi - \Delta\phi)\,dt. \qquad (10)$$

Angle ϕ, when used in (6) and (7), has the property of rotating the complex current vector I_2 to be 180 degrees out of phase with respect to the complex current vector I_1. This rotation process is shown graphically in Fig. 3. Here, the new position of the complex current vector of induction machine 2, I_{2rot}, is accomplished by rotating the complex vector I_2 by ϕ degrees. The reference frame of induction machine 1 remains fixed because the rotor flux angle θ_{rf1} was selected as the reference. In Fig. 3 there are three different reference systems: q_1d_1, which defines the position of induction machine 1, q_2d_2, which defines the position of induction machine 2, and $q_{2rot}d_{2rot}$, which defines the new position of the machine 2. Thus, it can be noted that in this new position, the complex current vectors I_1 and I_2 are 180 degrees out of phase. This an important result because if I_1 and I_2 have similar magnitudes, which is possible during normal drive operation, the elimination of the single-phase current through the DC-link capacitors can be achieved according to (1). Once ϕ is calculated by the PI-type controller in (10), it is utilized to generate the proper sets of reference currents in (4) and (5) for induction motor 2.

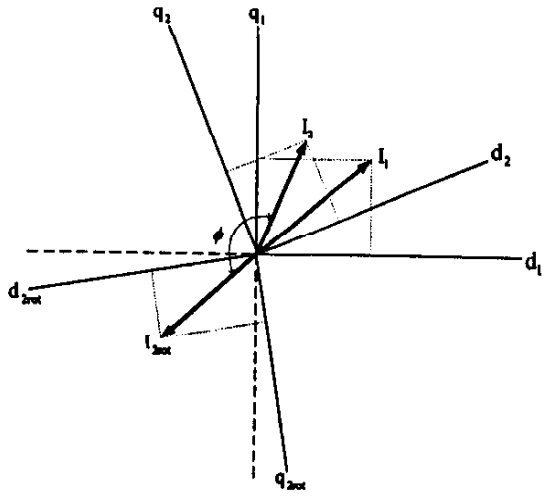

Fig. 3. Rotation of the reference frame of motor 2 by ϕ degrees with respect to the reference frame of motor 1.

IV. TRACTION APPLICATION OF THE PROPOSED DUAL DRIVE SYSTEM

Fig. 4 illustrates the general block diagram for the controls of the proposed drive system. The controls for induction motors 1 and 2 are developed utilizing Indirect Field-Oriented (IFO) control in the synchronous reference frame [9]. For an electric vehicle traction application, three driving situations are of interest: 1) the straight line regime, where both motors operate at the same speed, 2) the turning regime, where each machine operates at different speeds, and 3) slippage, where one of the induction motors holds almost zero load torque [10].

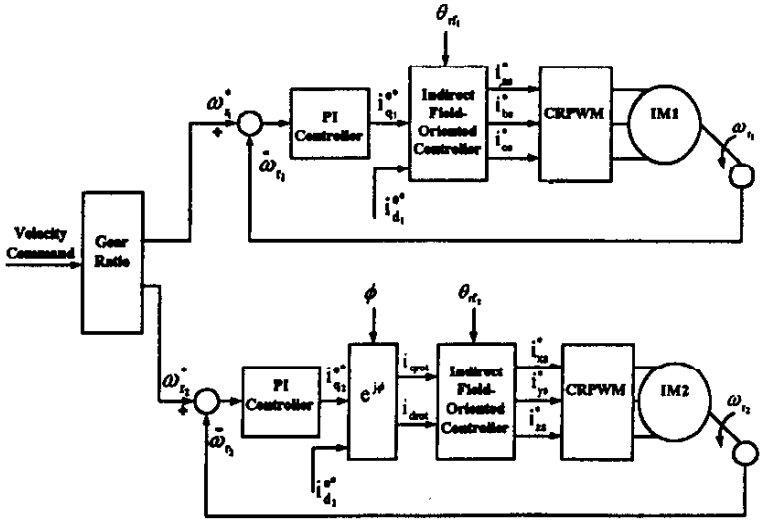

Fig. 4. General block diagram for the control of the proposed drive system.

A. Angular velocities of the two induction motors

In the block diagram of Fig.4, it is assumed that the vehicle total velocity (v) is maintained constant during each manuever. Then, the torque commands for the IFO control are produced by selecting the desired speed for the vehicle. Each induction motor of the proposed drive is utilized to drive one of the wheels of the traction axle. The angular speed for each motor depends on the type of driving regime selected. For the straight line regime, the angular speeds for each motor become

$$\omega_{r_1} = \omega_{r_2} = \frac{v}{Rw}. \tag{11}$$

For the turning regime, the angular speeds for each motor are different and expressed as

$$\omega_{r_1} = \frac{2v}{\left[1+\frac{R+\frac{W}{2}}{R-\frac{W}{2}}\right]Rw} \tag{12}$$

$$\omega_{r_2} = \frac{2v}{\left[1+\frac{R-\frac{W}{2}}{R+\frac{W}{2}}\right]Rw}. \tag{13}$$

Note that from (13) that the angular speed of induction motor 2 will be larger than the angular speed of induction motor 1.

B. Speed control of motor drive 1

The torque command for induction motor 1 is generated by a PI controller, which maintains constant speed under any load torque. The flux command becomes

$$i_{q_1}^{e*} = K_{pw}\left(\omega_{r_1}^{*} - \omega_{r_1}\right) + \frac{K_{iw}}{p}\left(\omega_{r_1}^{*} - \omega_{r_1}\right). \tag{14}$$

A constraint in the operation of the drive is that both motors must operate at the same frequency in order to minimize the ac current in the link capacitors. Fig. 5 shows the block diagram to determine the flux command for induction motor 1. To maintain the same frequencies in both induction motors, the necessary amount of flux Δi_d^{e*} is determined by the following expression:

$$\Delta i_d^{e*} = K_{pf}\left(\omega_{e_1} - \omega_{e_2}\right) + \frac{K_{if}}{p}\left(\omega_{e_1} - \omega_{e_2}\right) \tag{15}$$

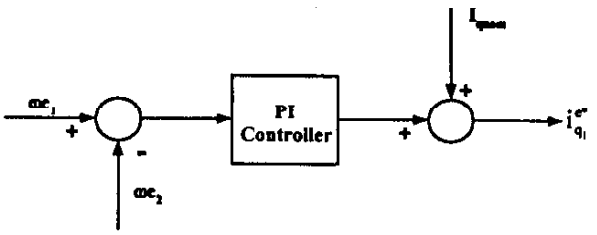

Fig. 5. Block diagram for generation of the flux command for induction motor 1, to maintain the same frequency in both machines.

Then, the differential flux Δi_d^{e*} is added to the nominal flux of induction motor 1. The final expression for the flux command becomes

$$i_{d_1}^{e*} = \Delta i_d^{e*} + I_{dnom} \tag{16}$$

where ω_{e_1} is the frequency of induction motor 1 and ω_{e_2} is the frequency of induction motor 2.

C. Speed control of motor drive 2

The speed control for induction motor 2 involves the generation of the torque command to maintain constant velocity. Its expression in the synchronous reference frame is

$$i_{q_2}^{e*} = -Kp_2(\omega_{r_2}^{*} - \omega_{r2}) + \frac{Ki_2}{p}(\omega_{r_2}^{*} - \omega_{r2}). \tag{17}$$

The flux command, $i_{d_2}^{e*}$, is maintained constant in its nominal value, 6 A. Both the flux and torque commands must be applied with negative signs. This will accomplish an out-of-phase angle of 180 degrees between the respective stator currents of both inverters. The strategy of eliminating the single-phase current through the DC-link capacitor is also contained in the control of induction motor 2, as seen in Fig. 4.

V. SIMULATION RESULTS

The proposed drive system has been simulated assuming two identical induction motors operating at the same fundamental frequency. In all simulations except the slippage condition, the induction motors operate under similar loads. The focus of this study is the analysis of the behavior of the DC-link circulating current through the

capacitors as the vehicle performs basic maneuvers. Therefore, for simplicity, the necessary torque to accelerate the vehicle and the torque to overcome the road load are modeled by a step torque. Three basic driving situations are simulated: straight-line, turning, and slippage. Primarily, the proposed drive system is simulated without control to minimize the DC-link capacitor currents.

A. Operation of the proposed drive without capacitor current control

Fig. 6 shows the current and voltage through DC-link capacitor 1 when the system is operating without any control. The circulation of single-phase currents is clearly seen. The current rises as high as the current of phase c (11.4 Apeak). In addition, due to this large capacitor current, large voltage oscillations can be seen through capacitor 1 (60 Vpeak). The same effect is produced in capacitor 2. Without utilizing any control method to reduce the voltage and current variations, the size of the DC-link capacitors would increase. Due to the increase in loss and larger capacitors, this would have a direct impact in the weight and cost of the drive. Therefore, the single-phase current flow in the DC-link must be eliminated or minimized for a practical application of the drive.

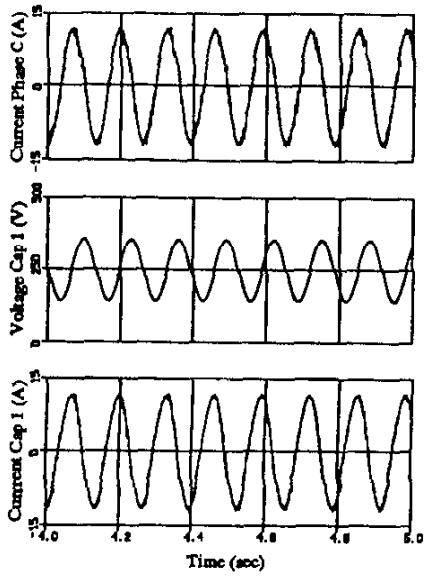

Fig. 6. Operation of the proposed drive system without control.

B. Straight-line Regime

During straight-line driving operation, each inductor motor operates with identical speeds as given by (11). Fig. 7 illustrates the current through capacitor 1. The simulation is carried out with a load of 4 N.m on each induction motor and a total vehicle velocity of 10 mph. It can be seen that at less than 2 seconds, the current reaches its steady state value. At this point, the current and voltage variations of the capacitor have been fully eliminated.

Fig. 8 demonstrates that if the load torque (rated torque) applied to each machine is increased, the minimization technique continues to be valid. Here, also, the current and the voltage through the capacitor are free of oscillations in the steady state. According to (1), to eliminate the currents through the DC capacitors, i_{cs} and i_{zs} must total zero. In addition, these currents must have similar magnitudes. Fig. 9 exhibits the currents of phase c and phase z. It can be seen that the current i_{zs} increases its phase until it becomes 180 degrees out of phase with respect to the current in phase c. This rotation is actively accomplished by feeding the angle given by (10) into the general block diagram of Fig 4. Because an electric vehicle will perform primarily in the straight-line regime, in which there is complete elimination of the DC-link capacitor currents, the proposed drive system is attractive for this traction application.

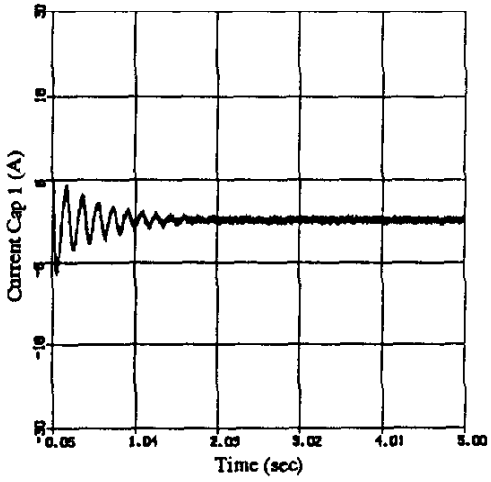

Fig. 7. Straight-line regime: DC-link capacitor current with the same load (4 N.m) and same speed (36 rad/sec) in both motors.

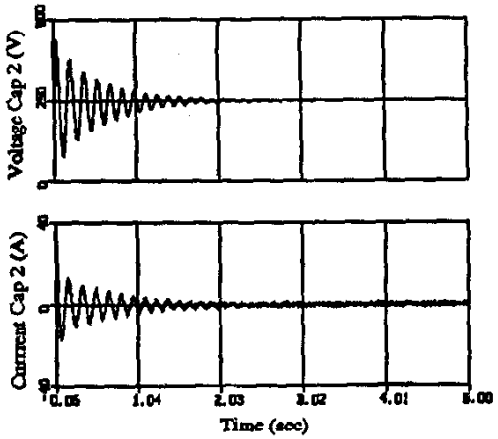

Fig. 8. Straight-line regime: DC-link capacitor voltage and current (12 N.m, 36 rad/sec for both motors).

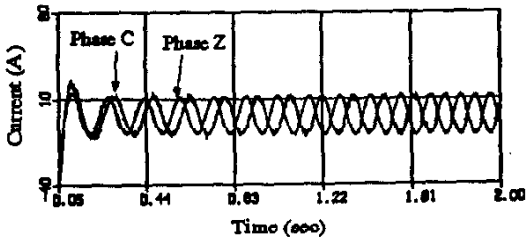

Fig. 9. Straight-line regime: current of phase c and z, 180 out of phase

C. Turning Regime

It is clear that the speeds of the motors are different for the turning condition. Given the total speed of the vehicle, the angular velocities of the motors are determined by (12) and (13). Fig. 10(a) shows that the proposed drive is capable of operating at different speeds and eliminating the single-phase current flow, as shown in 10(b). For this case, each induction motor operates with the same load torque (rated torque), and due to the restriction of equal frequency, each induction motor must operate with different slip and speed.

In sum, the turning regime simulations demonstrate that when both motor drives are operated approximately with the same current level, the problem of single-phase circulating current through the DC-link and voltage fluctuations can still be eliminated. It was found that aside from the difference in phase, the corresponding line current phases (e.g., c and z) remain nearly the same (1 A difference) for this condition. This represents a reduction of approximately 91% of the current through the capacitors without any control.

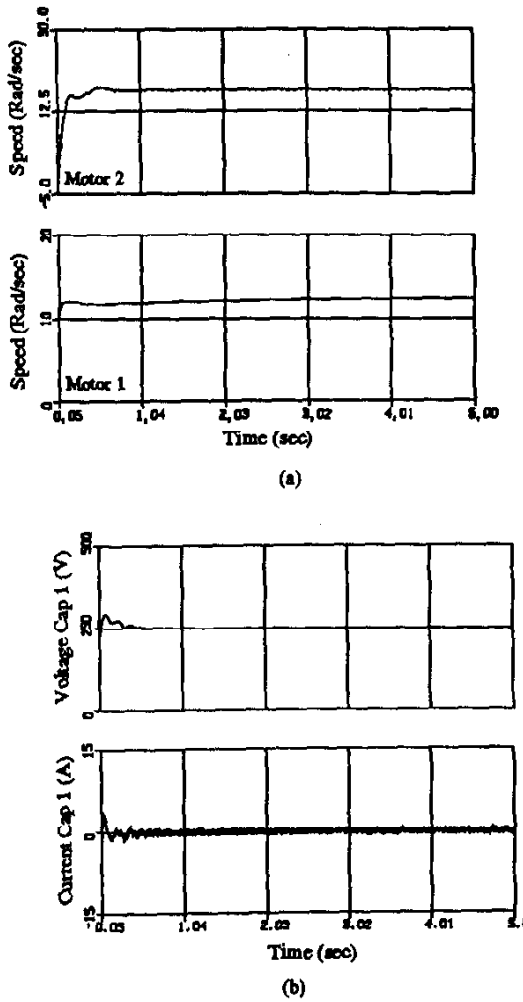

Fig. 10. Performance of the proposed drive system when operating under different speeds and same load torque (12 N.m): (a) the two motor speeds, (b) current and voltage capacitors.

D. Wheel Slippage

One special operational condition for the drive is when one of the wheels has full traction and the other has lost almost all traction capability. This operational condition, though a rare driving situation, is important to analyze in order to determine the limitations of the drive. The simulation of wheel slippage is accomplished by applying 1 N.m on motor 1 and 12 N.m on motor 2. During the slippage condition, it is assumed that the vehicle is turning with a curve radius of 4.8 meters at a constant speed of 10 mph. Fig. 11 illustrates the capacitor

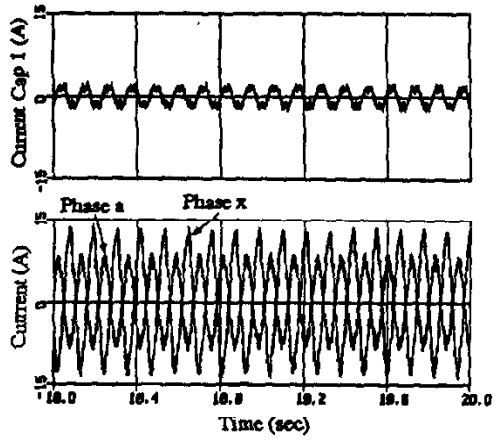

Fig. 11. Response of capacitor and phase currents a and x during wheel slippage.

current and voltage during the slippage operation. The currents of phase a and phase x are also shown. Due to the different load torques, it was found that the current in phase x becomes 3 A larger than the current of phase a. As a result, the difference in phase currents appears in the DC-link, which represents approximately 25% of the current of the DC-link without control. Thus, the voltage oscillations are approximately 50% of the actual value without control. Although the elimination of the circulating current through the DC capacitor is not complete, 75% of the current is eliminated, compared to the case without control. This driving situation also would be a worst case scenario for the operation of the proposed drive system.

VI. CONCLUSIONS

A dual three-phase motor drive system based on multiple two-phase PWM inverters has been proposed. The proposed drive system is capable of eliminating the single-phase circulation current through the DC-link capacitors. It has been shown that the elimination of the single-phase current, when applied to electric vehicle traction in the normal driving regimes, can be achieved by controlling the phase angle of the commanded currents to each inverter. This is accomplished without any additional hardware to that required for normal operation. The elimination of the circulating current reduces the overall losses, eliminates DC voltage variations and has relevant impact in reducing the cost and weight of the drive. An appropriate control model for vehicle traction application has been developed and simulated, demonstrating that the proposed drive system is a suitable alternative to conventional six switch inverter drives.

APPENDIX A

i^*_{as}	reference current phase a
i^*_{bs}	reference current phase b
i^*_{xs}	reference current phase x
i^*_{ys}	reference current phase y
$i^{e*}_{q_1}$	torque command, motor 1
$i^{e*}_{q_2}$	torque command, motor 2
$i^{e*}_{d_1}$	flux command, motor 1
$i^{e*}_{d_2}$	flux command, motor 2
I_1	magnitude current, motor 1
I_2	magnitude current, motor 2
I_{qnom}	nominal value of i_q
θ_{rf1}	rotor flux position, motor 1
θ_{rf2}	rotor flux position, motor 2
p	differential operator d/dt
ω_{r1}	angular speed, motor 1
ω_{r2}	angular speed, motor 2
$\omega^*_{r_1}$	angular speed reference, motor 1
$\omega^*_{r_2}$	angular speed reference, motor 2

APPENDIX B

Machine Parameters

3 Hp, 3ϕ	L_m=0.070 H
220 V	L_r=0.072 H
8.08 A	L_s=0.072 H
4-poles	r_r=0.81 Ω
I_{qnom}=6 A	r_s=0.50 Ω

APPENDIX C

Controller Parameters

$K_{p\phi}$=3.0	$K_{p\phi}$=8.0
K_{pw}=5.0	K_{iw}=1.8
K_{pf}=0.02	K_{if}=1.5
K_{p2}=1.0	K_{i2}=1.5
R=4.8 m	v=10 mph
W=1.5 m	R_w=0.3 m

REFERENCES

[1] J. F. Eastham, A. R. Daniels, and R. T. Lipcynski, "A novel power inverter configuration," in *Conference Records IEEE/IAS Annual Meeting*, pp. 748-751, 1980.

[2] H. W. Van Der Broeck and J. D. Van Wyk, "A comparative investigation of a three-phase induction machine with a component minimized voltage-fed inverter under different control options," *IEEE Transactions on Industry Applications*, vol. IA-20, no. 2, pp. 309-320, March/April 1984.

[3] H. W. Van Der Broeck and H. C. Skudelny, "Analytical analysis of the harmonic effects of a PWM ac drive," *IEEE Transactions on Power Electronics*, vol. PE-3, no. 2, pp. 216-223, April 1988.

[4] G. T. Kim and T. A. Lipo, "VSI-PWM rectifier/inverter system with a reduced switch count," *IEEE Transactions on Industry Applications*, vol. IA-32, no. 6, pp. 1331-1337, Nov./Dec. 1996.

[5] F. Blaabjerg, S. Freysson, H.-H. Hansen, and S. Hansen, "A new optimized space vector modulation strategy for a component minimized voltage source inverter," *Applied Power Electronics Conference and Exposition*, vol. 2, pp. 577-585, 1995.

[6] F. B. Blaabjerg, D. Neacsu, and J. K. Pedersen, "Adaptive SVM to compensate dc-link voltage ripple for component minimized voltage source inverter," *Proceedings on IEEE PESC*, pp. 580-589, 1997.

[7] A. Bouscayrol, M. Pietrzak-David, and B. de Fornel, "Comparative studies of inverter structures for a mobile robot asynchronous motorisation," *IEEE International Symposium on industrial Electronics*, pp. 447-452, 1996.

[8] G. T. Kim and T. A. Lipo, "DC Link voltage control of reduced switch VSI-PWM rectifier/inverter system," *Proceedings of the IECON 97*, vol. 2, pp. 833-838, 1997.

[9] D. W. Novotny and T. A. Lipo, *Vector Control and Dynamics of AC Drives*, Oxford: New York, 1997.

[10] P. M. Kelecy, "Control methodologies for single inverter, dual induction motor drives for electric vehicles," Ph.D. Dissertation, University of Wisconsin-Madison, 1995.